

Dynamics of quantum discord and geometric quantum discord in multiqubit interacting system

Xiao-Di Cheng(程晓迪), Ya-Jun Zheng(郑雅君), Meng-Jie Ran(冉梦杰), and Xiao-Yun Wang(王小云)

Citation: Chin. Phys. B, 2025, 34 (**5**): 050309. DOI: 10.1088/1674-1056/adca16
Journal homepage: http://cpb.iphy.ac.cn; http://iopscience.iop.org/cpb

What follows is a list of articles you may be interested in

Sudden change of interferometric power for X-shape states

Dian Zhu(朱典), Fu-Lin Zhang(张福林), and Jing-Ling Chen(陈景灵)
Chin. Phys. B, 2025, 34 (**2**): 020305. DOI: 10.1088/1674-1056/ad9732

Quantum discord and its dynamics for multipartite systems

Jiaxin Luo(罗嘉欣) and Qiong Guo(郭琼)
Chin. Phys. B, 2024, 33 (**6**): 060303. DOI: 10.1088/1674-1056/ad3810

Quantum correlation enhanced bound of the information exclusion principle

Jun Zhang(张钧), Kan He(贺衍), Hao Zhang(张昊), and Chang-Shui Yu(于长水)
Chin. Phys. B, 2023, 32 (**9**): 090301. DOI: 10.1088/1674-1056/accf80

Quantum correlation and entropic uncertainty in a quantum-dot system

Ying-Yue Yang(杨颖玥), Li-Juan Li(李丽娟), Liu Ye(叶柳), and Dong Wang(王栋)
Chin. Phys. B, 2022, 31 (**10**): 100303. DOI: 10.1088/1674-1056/ac7295

Protecting geometric quantum discord via partially collapsing measurements of two qubits in multiple bosonic reservoirs

Xue-Yun Bai(白雪云) and Su-Ying Zhang(张素英)
Chin. Phys. B, 2022, 31 (**4**): 040308. DOI: 10.1088/1674-1056/ac4f54

SPECIAL TOPIC — Quantum communication and quantum network

Dynamics of quantum discord and geometric quantum discord in multiqubit interacting system

Xiao-Di Cheng(程晓迪), Ya-Jun Zheng(郑雅君), Meng-Jie Ran(冉梦杰), and Xiao-Yun Wang(王小云)†

College of Physics Mechanical and Electrical Engineering, Jishou University, Jishou 416000, *China*

(Received 21 November 2024; revised manuscript received 6 April 2025; accepted manuscript online 8 April 2025)

Using quantum discord (QD) and geometric quantum discord (GQD), quantum correlation dynamics is investigated for two coupled qubits within a multiqubit interacting system in the zero-temperature bosonic reservoir, under both weak and strong qubit-reservoir coupling regimes. The multiqubit system is connected with either a common bosonic reservoir (CBR) or multiple independent bosonic reservoirs (IBRs). In the CBR case, our findings indicate that both QD and GQD can be strengthened by increasing the number of qubits in the multiqubit system. Furthermore, we study the steady state QD and GQD in the strong coupling regime, and find that the stable value in the long-time limit is determined exclusively by the number of qubits. The evolution period of QD and GQD gets longer as the dipole–dipole interaction (DDI) strength increases, which helps prolong the correlation time and thus preserves the quantum correlation under the weak coupling regime. Further analysis reveals notable differences between the CBR and IBRs scenarios. In the IBRs case, the decay of QD and GQD becomes slower compared to the CBR case, with both measures tending to zero at a reduced rate. Moreover, GQD consistently exhibits lower values than QD in both scenarios. These findings provide valuable insights into the selection of appropriate correlation measurement techniques for quantifying quantum correlations.

Keywords: quantum discord, geometric quantum discord, quantum correlation dynamics, multiqubit system

PACS: 03.65.Ta, 03.65.Yz, 03.67.Pp

DOI: 10.1088/1674-1056/adca16 **CSTR:** 32038.14.CPB.adca16

1. Introduction

The quantification of quantum correlations is vital for the swift progression of quantum technologies. Various measurements of quantum correlations have been proposed, including quantum entanglement,[1] quantum discord (QD)[2] and quantum coherence.[3] In addition to quantum entanglement, QD can exist in separable mixed states exhibiting nonclassical correlations, serving as a more fundamental quantum resource than entanglement.[4–6] This characteristic makes QD pivotal in various quantum information tasks, including quantum teleportation,[7–9] quantum computing,[10,11] quantum communication,[12,13] quantum many-body systems,[14–16] etc. Despite its extensive applications, both QD and other forms of quantum correlations are inherently fragile. The inevitable interactions with the environment induce the decoherence of the system,[17] presenting a significant obstacle to the advancement of quantum technologies. It has been proposed that environments can be utilized to restore or preserve QD under specific conditions. Consequently, exploring the impact of decoherence on QD, identifying effective methods to eliminate or at least reduce the effect of decoherence, and regulating the environment to protect QD hold significant practical relevance.

As a novel measure of quantum correlation, QD was first proposed by Ollivier and Zurek,[2] and later analyzed by Vedral *et al.*[18] In general, due to the complexity of the optimization, it is hard to obtain the exact analytical solution of QD for arbitrary state in bipartite system. For this reason, Dakić et al. introduced geometric quantum discord (GQD) based on the Hilbert–Schmidt norm.[19] Although GQD provides a simpler computational approach than QD, it exhibits limitations in fully capturing quantum correlations under certain local operations.[20–22] It is necessary to discuss which measurement method to select appropriately in the multiqubit interacting system. In recent decades, significant theoretical and experimental advancements have underscored the pivotal role of quantum correlations in multipartite quantum systems.[23–25] Previous studies have explored the interaction between two qubits with either a common reservoir or independent reservoirs, employing the second-order time-convolutionless master equations.[26,27] Additionally, research on steady-state entanglement and coherence in two coupled qubits within independent reservoirs has yielded significant insights.[28] In multiqubit-interacting systems, the single-excitation dynamics of N-qubit in a common non-Markovian reservoir was discussed.[29,30] Furthermore, researchers explored the entanglement generation in an N-atoms system under the weak coupling regime,[31] and the enhancement of quantum coherence in multiqubit-interacting systems was investigated.[32]

In this work, we investigate the dynamics of QD and

†Corresponding author. E-mail: wxyyun@163.com

© 2025 Chinese Physical Society and IOP Publishing Ltd. All rights, including for text and data mining, AI training, and similar technologies, are reserved.

GQD in an N-qubit system with dipole–dipole interactions (DDI), which is connected to either a common bosonic reservoir (CBR) or independent bosonic reservoirs (IBRs) in the single-excitation regime. This multiqubit interacting system can be realized in various experimental setups, including quantum dots,[33–35] superconducting networks,[36–38] cold atoms[39,40] and transmon qubits.[41,42] Therefore, the model we have selected is instrumental in comprehending the correlation dynamics of qubit systems across a variety of environments, including finite-temperature vibronic environments and quantized electromagnetic field reservoirs.[43–46] Recent advancements in the study of QD dynamics in multiqubit systems demonstrate that QD offers significant insights into quantum correlations.[47–49] Although QD serves as an original measure of quantum correlations, its ability to fully capture the intricate dynamics of correlation in multiqubit systems remains limited. The dynamics of QD and GQD in two-qubit states within multiqubit interacting systems remain understudied. This gap underscores the importance of selecting appropriate methods to quantify correlation dynamics. In the subsequent analysis, we thus examine the effects of complex environments on the correlation dynamics of QD and GQD by varying the total number of qubits and the DDI strength within the multiqubit system under both weak and strong coupling regimes. As demonstrated subsequently, it becomes evident that QD and GQD of the two-qubit system can be strengthened by enhancing the number of qubits, which contrasts sharply with the influence of the DDI between the qubits.

This research is structured as follows. Section 2 introduces the physical model and investigates the dynamical evolution of quantum correlations in the multiqubit interacting system. A brief review of QD and GQD measures of quantum correlations is also provided. Section 3 presents a detailed analysis of the results of QD and GQD in the CBR and IBRs cases. Finally, the findings of this study are summarized in Section 4.

2. Model and its exact solution

2.1. Multiqubit-interacting system in a CBR

First, we consider a system of N qubits in a common zero-temperature bosonic reservoir, where all qubits are coupled to the reservoir with the same coupling strength. The qubits connect with each other via DDI. Under the rotating wave approximation, the total Hamiltonian including the qubit system, reservoir, and the interaction part is of the form[50]

$$H = H_{\mathrm{S}} + H_{\mathrm{R}} + H_{\mathrm{I}}, \tag{1}$$

where

$$\begin{aligned} H_{\mathrm{S}} &= \frac{\omega_0}{2}\sum_{j=1}^{N}\sigma_j^z, \\ H_{\mathrm{R}} &= \sum_k \omega_k a_k^+ a_k, \\ H_{\mathrm{I}} &= \mathrm{i}\sum_{j,k} g_k\left(\sigma_j^+ a_k - \sigma_j^- a_k^+\right) + \sum_{j\neq l} J\sigma_j^+\sigma_l^-. \end{aligned} \tag{2}$$

Here, the parameter a_k^+ (a_k) denotes the creation (annihilation) operator of the kth mode in the bosonic field, $\sigma_j^{x,y,z}$ is the Pauli matrix of the jth qubit, the ladder operator of the jth qubit is $\sigma_j^{\pm} = \frac{1}{2}\left(\sigma_j^x \pm \sigma_j^y\right)$, and ω_0 and ω_k are the transition frequency of the qubits and the kth bosonic reservoir mode, respectively. g_k is the coupling strength between the qubit system and the bosonic reservoir. J is the DDI strength between the qubits.

It is obvious that the Hamiltonian conserves the excitation number, which means that it commutes with the number operator $\hat{N} = \sum_{j=1}^{N}\sigma_j^+\sigma_j^- + \sum_k a_k^+ a_k$. In this way, we consider solving the dynamics of the system in the single-excitation subspace, which makes the model numerically solvable. In the interaction picture, the interaction Hamiltonian H_{I} can be expressed as

$$\begin{aligned} \tilde{H}_{\mathrm{I}} =\ & \mathrm{i}\sum_{j,k} g_k\left(\sigma_j^+ a_k\,\mathrm{e}^{\mathrm{i}(\omega_0-\omega_k)t} - \sigma_j^- a_k^+\,\mathrm{e}^{-\mathrm{i}(\omega_0-\omega_k)t}\right) \\ & + \sum_{j\neq l} J\sigma_j^+\sigma_l^-. \end{aligned} \tag{3}$$

When the entire system is treated as closed, its dynamical evolution is governed by the Schrödinger equation. To solve the Schrödinger equation, we consider the initial joint system-reservoir state to be

$$|\psi(0)\rangle = c_0|\varphi_0\rangle + \sum_{j=1}^{N} c_j(0)|\varphi_j\rangle + \sum_k c_k(0)|\varphi_k\rangle, \tag{4}$$

where $|\varphi_0\rangle = |0\rangle_{\mathrm{S}}\otimes|0\rangle_{\mathrm{R}}$ is the ground state of the entire system. $|\varphi_j\rangle = |j\rangle_{\mathrm{S}}\otimes|0\rangle_{\mathrm{R}}$ represents the jth qubit in its excited state and all the other qubits and reservoirs in the ground state. $|\varphi_k\rangle = |0\rangle_{\mathrm{S}}\otimes|1_k\rangle_{\mathrm{R}}$ denotes all qubits in their ground state and the bosonic reservoir with only one excitation in the kth field mode. The joint state at generic time of the system is given by

$$|\psi(t)\rangle = c_0|\varphi_0\rangle + \sum_{j=1}^{N} c_j(t)|\varphi_j\rangle + \sum_k c_k(t)|\varphi_k\rangle. \tag{5}$$

For convenience, we introduce the parameter $c_+(t) = \sum_{j=1}^{N} c_j(t)$ to represent the total excited-state amplitude. Substituting Eq. (5) into the Schrödinger equation, we obtain a set of coupled differential equations for the amplitudes as follows:

$$\begin{aligned} \dot{c}_j &= -\mathrm{i}J(c_+ - c_j) + \sum_k c_k g_k\,\mathrm{e}^{\mathrm{i}(\omega_0-\omega_k)t}, \\ \dot{c}_+ &= -\mathrm{i}J(N-1)c_+ + N\sum_k c_k g_k\,\mathrm{e}^{\mathrm{i}(\omega_0-\omega_k)t}, \\ \dot{c}_k &= -g_k\,\mathrm{e}^{-\mathrm{i}(\omega_0-\omega_k)t}c_+. \end{aligned} \tag{6}$$

We assume that initially the bosonic field is in its vacuum configuration, $c_k(0) = 0$, integrating the differential equation for

c_k, we arrive at

$$c_k(t) = -\int_0^t \mathrm{d}t_1 g_k \mathrm{e}^{-\mathrm{i}(\omega_0-\omega_k)t_1} c_+(t_1). \tag{7}$$

In the continuum limit for the bosonic reservoir, we can introduce the spectral density $J(\omega)$ through

$$\sum_k g_k^2 \mathrm{e}^{\mathrm{i}(\omega_0-\omega_k)t} = \int \mathrm{d}\omega J(\omega) \mathrm{e}^{\mathrm{i}(\omega_0-\omega)t}. \tag{8}$$

Thus, we define the memory kernel as the Fourier transform of the spectral density, namely,

$$G(t) = \int \mathrm{d}\omega J(\omega) \mathrm{e}^{\mathrm{i}(\omega_0-\omega)t}, \tag{9}$$

then we substitute Eq. (7) into Eq. (6), and obtain

$$\begin{aligned}
\dot{c}_j &= -\mathrm{i}J(c_+ - c_j) - \int_0^t \mathrm{d}t_1 G(t-t_1) c_+(t_1), \\
\dot{c}_+ &= -\mathrm{i}J(N-1)c_+ - N\int_0^t \mathrm{d}t_1 G(t-t_1) c_+(t_1),
\end{aligned} \tag{10}$$

which can be solved via the Laplace transform of the single qubit amplitude c_j and the total excited-state amplitude c_+. We thus get

$$\begin{aligned}
\tilde{c}_j(s) &= \frac{c_j(0)}{s-\mathrm{i}J} - \frac{c_+(0)\left(\tilde{G}(s)+\mathrm{i}J\right)}{(s-\mathrm{i}J)\left[s+\mathrm{i}J(N-1)+N\tilde{G}(s)\right]}, \\
\tilde{c}_+(s) &= \frac{c_+(0)}{s+\mathrm{i}J(N-1)+N\tilde{G}(s)},
\end{aligned} \tag{11}$$

where $\tilde{G}(s)$ is the Laplace transform of the memory kernel. For convenience, we consider the reservoir spectral density $J(\omega)$ to be of Lorentzian form in the following, i.e.,

$$J(\omega) = \frac{1}{2\pi} \frac{\gamma_0 \lambda^2}{(\omega-\omega_0)^2+\lambda^2}, \tag{12}$$

where γ_0 serves as the qubit-reservoir coupling strength, which is the inverse of the system relaxation time. λ is the spectral width, and we utilize the qubits transition frequency ω_0 as the reservoir center frequency. Therefore, the amplitude $c_j(t)$ of the jth qubit can be solved by the inverse Laplace transformation as

$$\begin{aligned}
c_j(t) = &\left(c_j(0) - \frac{c_+(0)}{N}\right)\mathrm{e}^{\mathrm{i}Jt} + \frac{c_+(0)}{N}\left[\mathrm{e}^{-\frac{\lambda+\mathrm{i}J(N-1)}{2}t}\right. \\
&\left.\times\left(\cosh\left(\frac{\sigma_1}{2}t\right) + \frac{\lambda-\mathrm{i}J(N-1)}{\sigma_1}\sinh\left(\frac{\sigma_1}{2}t\right)\right)\right],
\end{aligned} \tag{13}$$

where $\sigma_1 = \sqrt{(\lambda-\mathrm{i}J(N-1))^2 - 2\gamma_0\lambda N}$. The parameters λ and γ_0 can distinguish the Markovian and non-Markovian regimes. The dynamics of the two-qubit system is Markovian under the weak coupling condition $\lambda > 2\gamma_0$, while it becomes non-Markovian when $\lambda < 2\gamma_0$. From the expression of $c_j(t)$, we emphasize that the correlation dynamics behaviors of the system can be modified by the number N of qubits and the DDI strength J between the qubits in the weak ($\lambda > 2\gamma_0$) or strong ($\lambda < 2\gamma_0$) system-environment coupling regimes.

2.2. Multiqubit interacting system in IBRs

The second condition we consider is that the N DDI qubits are embedded in individual bosonic reservoirs. We assume that the local environments surrounding the multiqubit system are sufficiently distinct, such that inter-environment correlations of different qubits are negligible. Such models are employed in the light-harvesting complexes for energy transfer.[51–54] The interaction Hamiltonian in the interaction picture then becomes

$$\begin{aligned}
\tilde{H}_{\mathrm{I}} = &\ \mathrm{i}\sum_{j,k} g_k \left(\sigma_j^+ a_{jk} \mathrm{e}^{\mathrm{i}(\omega_0-\omega_k)t} - \sigma_j^- a_{jk}^+ \mathrm{e}^{-\mathrm{i}(\omega_0-\omega_k)t}\right) \\
&+ \sum_{l\neq j} J\sigma_j^+\sigma_l^-,
\end{aligned} \tag{14}$$

where we assume each reservoir has the same spectral density, a_{jk} (a_{jk}^+) represents the annihilation (creation) operator for the kth field mode with coupling strength g_k of the jth qubit's reservoir. As such we have the joint state at generic time of the system,

$$|\psi(t)\rangle = c_0|\varphi_0\rangle + \sum_{j=1}^N c_j(t)|\varphi_j\rangle + \sum_{jk} c_{jk}(t)|\varphi_{jk}\rangle, \tag{15}$$

where $|\varphi_{jk}\rangle$ denotes the excitation state in mode k of the jth qubit's reservoir. The set of coupled differential equations is then

$$\begin{aligned}
\dot{c}_j &= -\mathrm{i}J(c_+ - c_j) + \sum_k c_{jk} g_k \mathrm{e}^{\mathrm{i}(\omega_0-\omega_k)t}, \\
\dot{c}_+ &= -\mathrm{i}J(N-1)c_+ + \sum_{jk} c_{jk} g_k \mathrm{e}^{\mathrm{i}(\omega_0-\omega_k)t}, \\
\dot{c}_{jk} &= -g_k \mathrm{e}^{-\mathrm{i}(\omega_0-\omega_k)t} c_j.
\end{aligned} \tag{16}$$

Integrating c_{jk} with $c_{jk}(0) = 0$ and substituting back into Eq. (16), we obtain

$$\begin{aligned}
\dot{c}_j &= -\mathrm{i}J(c_+ - c_j) - \int_0^t \mathrm{d}t_1 G(t-t_1) c_j(t_1), \\
\dot{c}_+ &= -\mathrm{i}J(N-1)c_+ - \int_0^t \mathrm{d}t_1 G(t-t_1) c_+(t_1).
\end{aligned} \tag{17}$$

Then we can determine the Laplace transform solutions through Eq. (17),

$$\begin{aligned}
\tilde{c}_+(s) &= \frac{c_+(0)}{s+\mathrm{i}J(N-1)+\tilde{G}(s)}, \\
\tilde{c}_j(s) &= \frac{c_j(0)}{s-\mathrm{i}J+\tilde{G}(s)} \\
&\quad - \frac{\mathrm{i}Jc_+(0)}{\left[s-\mathrm{i}J+\tilde{G}(s)\right]\left[s+\mathrm{i}J(N-1)+\tilde{G}(s)\right]}.
\end{aligned} \tag{18}$$

In the same way, for the IBRs case, we obtain the amplitude of the jth qubit $c_j(t)$,

$$\begin{aligned} c_j(t) &= \left(c_j(0)-\frac{c_+(0)}{N}\right)\mathrm{e}^{-\frac{\lambda-\mathrm{i}J}{2}t} \\ &\times\left[\cosh\left(\frac{\sigma_2 t}{2}\right)+\sinh\left(\frac{\sigma_2 t}{2}\right)\frac{\lambda+\mathrm{i}J}{\sigma_2}\right] \\ &+\frac{c_+(0)}{N}\mathrm{e}^{\frac{-[\lambda+\mathrm{i}J(N-1)]}{2}t} \\ &\times\left[\cosh\left(\frac{\sigma_3 t}{2}\right)+\sinh\left(\frac{\sigma_3 t}{2}\right)\frac{\lambda-\mathrm{i}J(N-1)}{\sigma_3}\right], \end{aligned} \tag{19}$$

where

$$\sigma_2=\sqrt{(\lambda+\mathrm{i}J)^2-2\gamma_0\lambda},\quad \sigma_3=\sqrt{[\lambda-\mathrm{i}J(N-1)]^2-2\gamma_0\lambda}.$$

In our study, we mainly focus on the QD and GQD dynamics of the two-qubit system (i.e., the jth and lth qubits). By tracing the other DDI qubits and the reservoirs, the reduced density matrix $\rho^{j,l}$ of the two-qubit system in the basis $\{|e,e\rangle,|e,g\rangle,|g,e\rangle,|g,g\rangle\}$ is given by

$$\rho^{j,l}=\begin{pmatrix} 0 & 0 & 0 & 0 \\ 0 & |c_j|^2 & c_j c_l^* & 0 \\ 0 & c_j^* c_l & |c_l|^2 & 0 \\ 0 & 0 & 0 & 1-|c_j|^2-|c_l|^2 \end{pmatrix}. \tag{20}$$

We select the maximally entangled Bell state $|\varphi(0)\rangle=(1/\sqrt{2})(|e,g\rangle+|g,e\rangle)$ as the initial state of the two-qubit system, such that the initial amplitudes of the two qubits are $c_1(0)=c_2(0)=1/\sqrt{2}$, the remaining $N-2$ qubits and reservoirs are in their ground states. Therefore, QD and GQD are theoretically equal to 1 at the initial time, which implies that the two-qubit system has the maximum quantum correlations.

2.3. Measures of quantum correlations

For bipartite systems, the best-known measure of nonclassical correlation is QD, which is defined as the difference between quantum mutual information and classical correlation. From Eq. (20), we can obtain the analytical expression of QD for the X-form state as follows:[55,56]

$$D\left(\rho^{j,l}\right)=\min\left\{D_1\left(\rho^{j,l}\right),D_2\left(\rho^{j,l}\right)\right\}, \tag{21}$$

where $D_1\left(\rho^{j,l}\right)=H(\rho_{11}+\rho_{22})+\sum_{i=1}^{4}\lambda_i\log_2\lambda_i+H(\alpha)$, $D_2\left(\rho^{j,l}\right)=\sum_{i=1}^{4}\lambda_i\log_2\lambda_i-\sum_{i=1}^{4}\rho_{ii}\log_2\rho_{ii}$, λ_i is the eigenvalue of the reduced density matrix $\rho^{j,l}$, $H(x)=-x\log_2 x-(1-x)\log_2(1-x)$ represents the Shannon entropy and $\alpha=\frac{1}{2}\left[1+\sqrt{[1-2(\rho_{33}+\rho_{44})]^2+4(|\rho_{23}|+|\rho_{14}|)^2}\right]$.

Another quantification of quantum correlation is GQD, which is defined as the minimum Hilbert–Schmidt distance between a given state and the set of zero discord states.[19] For the two-qubit state $\rho^{j,l}(t)$ with the X-structured matrix, GQD can be calculated analytically as[57]

$$D^2(\rho^{j,l})=\frac{1}{2}(2\alpha_1+\alpha_2-\max\{\alpha_1,\alpha_2\}), \tag{22}$$

where

$$\alpha_1=2|\rho_{23}|^2,\quad \alpha_2=\rho_{33}^2+(\rho_{22}-\rho_{44})^2. \tag{23}$$

In the following analysis, we employ Eqs. (21) and (22) to investigate how the number of qubits and the DDI between the qubits affect the correlation dynamics of QD and GQD in both weak and strong coupling regimes.

3. Results and discussion

In this section, we study the QD and GQD of two coupled qubits within the multiqubit system that are immersed in CBR or IBRs cases. We depict the dynamics of the system in terms of the given reduced density matrix $\rho^{j,l}$. In the following, we concentrate on the effects of the number of the qubits N and the DDI strength J on QD and GQD under both weak (Markovian) and strong (non-Markovian) system-environment coupling regimes.

3.1. QD and GQD dynamics in CBR case

We begin by considering the CBR case. The dynamic behaviors of QD (the blue solid line) and GQD (the red solid line) are depicted in Fig. 1 for different number of qubits N and DDI strength J under the weak coupling regime $\gamma_0=0.1\lambda$. In Figs. 1(a)–1(c), we fix $J=0$. Even in the absence of the DDI influence between the qubits, couplings between the multiqubit system and its environment still persist. In the condition of different number of qubits N, QD and GQD decay monotonically with the dimensionless time $\gamma_0 t$ and reach a steady value during the long time evolution process. The steady value increases with the number of qubits, which means that increasing N enhances the steady state QD and GQD of the two-qubit system. Furthermore, one can find that QD and GQD have the same trend but show different values under the same parameters of the system, and GQD is always smaller than QD. This demonstrates that QD better preserves quantum correlation than GQD in the multiqubit interacting system.

To find the influence of DDI strength J on QD and GQD, we further increase J to 0.5 as illustrated in Figs. 1(d)–1(f). In Fig. 1(d), the trends of QD and GQD remain unchanged when $N=2$. Notably, in contrast to the previous conditions depicted in Figs. 1(a)–1(c), both QD and GQD exhibit damped oscillations and asymptotically approach a stable value over a longer duration in Figs. 1(e) and 1(f). As N increases, the oscillation of both QD and GQD intensifies. By adding the DDI into the multiqubit system, we can obtain that it may

also show non-Markovian behavior even under the weak coupling regime. The increase of J may retard both QD and GQD loss during the evolution, leading to oscillatory decay with reduced attenuation, which helps prolong the quantum correlation time. Therefore, we observe that the presence of the DDI between the qubits can preserve the QD and GQD from the multipartite environmental effects.

Next, we examine how QD and GQD vary with the number of qubits and DDI strength under the strong coupling regime $\gamma_0 = 5\lambda$ as illustrated in Fig. 2. In this regime, the multiqubit system can always exhibit non-Markovian dynamics for any N with or without DDI J. It is evident that the non-Markovian behavior of QD and GQD displays both similarities and distinctions when compared to the case in Fig. 1. In Figs. 2(a)–2(c), after removing the DDI between the qubits and comparing the results to the weak coupling regime, QD and GQD exhibit an oscillatory trend over time before reaching a stable value. At the same time, both oscillation frequency and amplitude increase with the number of qubits N. In other words, a larger N enhances the non-Markovian behavior of the multiqubit system. However, as illustrated in Figs. 2(a) and 2(d), the survival time of QD and GQD is shorter than that in Figs. 1(a) and 1(d). This is because the increase in the value of γ_0 leads to more frequent information exchange between the qubits and the reservoir. When J is increased to 0.5 in Figs. 2(d)–2(f), the oscillation frequency increases but the amplitude decreases under the same number of qubits compared to the situation of $J = 0$. A comparison between Fig. 2 and Fig. 1 reveals that the effect of DDI strength J on QD and GQD in the multiqubit system is significantly weakened in the strong coupling regime compared to the weak coupling regime, where the strong interaction between the qubits and the reservoir becomes the dominant factor governing the dynamics. Similar to the weak coupling regime, GQD is always smaller than QD and both QD and GQD enter steady values over a long period of evolution.

To comprehend the impact of N and J on QD and GQD comprehensively, we present the steady state QD and GQD varying with N and J under the strong coupling regime $\gamma_0 = 5\lambda$ in Fig. 3. By fixing the DDI strength J as a constant, we can see that the steady values of GQD and QD strengthen as the number of qubits N increases, but the value of QD is always larger than that of GQD under the same N, which means that QD is more practical on improving quantum correlation than GQD in the multiqubit interacting system. However, when fixing N as a constant, the values for both GQD and QD remain invariant with the increase of J. The steady values of QD and GQD are independent of DDI strength J between the qubits and determined exclusively by the number of the qubits. That is to say, to preserve QD and GQD in the bipartite system within the multiqubit system, a large number of qubits are essential. Moreover, as shown in Figs. 1 and 2, regardless of whether the system is in weak or strong coupling regime, a larger steady value of QD and GQD can be obtained when a larger N is introduced. By increasing the number of qubits within the multiqubit system, we can reduce the effect of the reservoir on individual qubits.

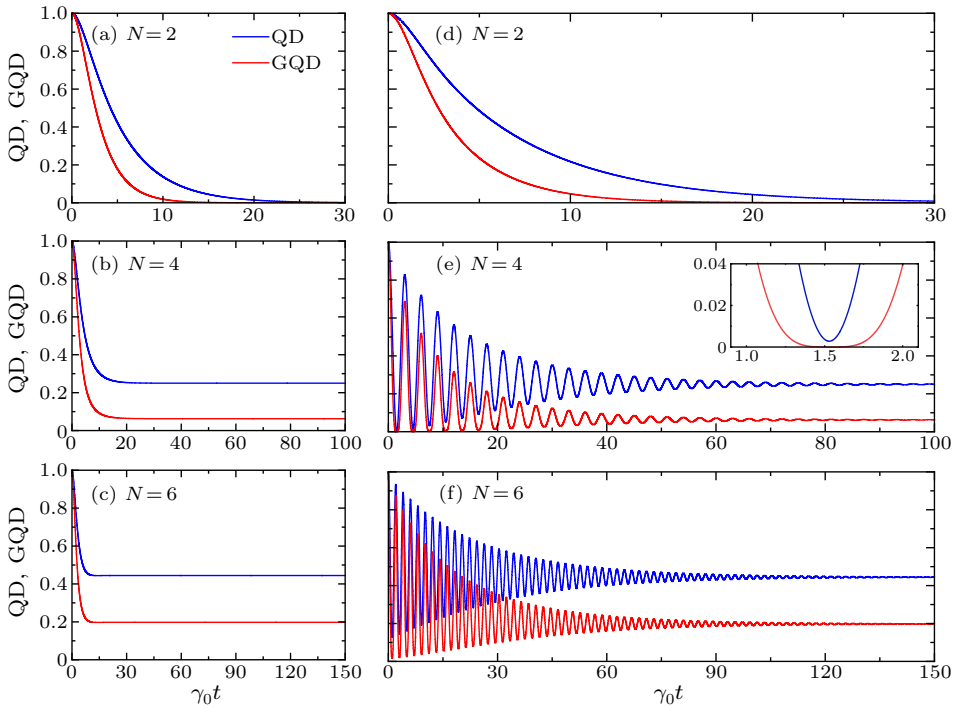


Fig. 1. (a)–(c) Under the weak coupling regime ($\gamma_0 = 0.1\lambda$), QD (blue solid line) and GQD (red solid line) versus $\gamma_0 t$ for $J = 0$, with $N = 2, 4, 6$, respectively. (d)–(f) Same as the left panel but for $J = 0.5$.

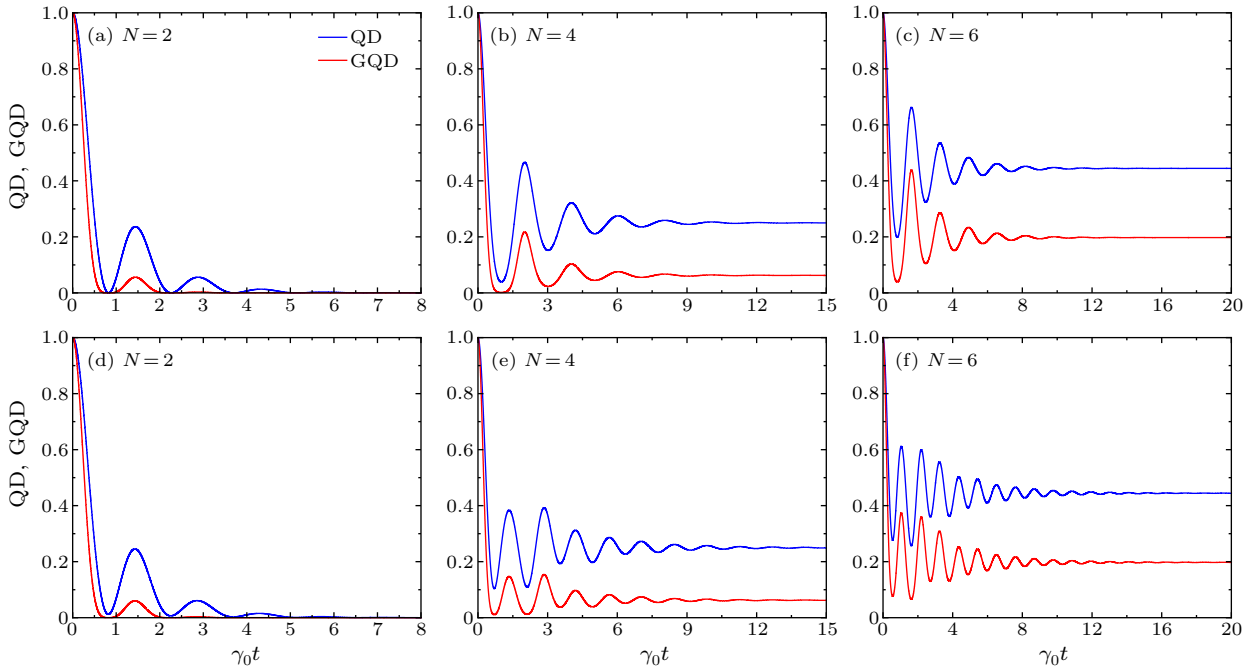


Fig. 2. (a)–(c) Under the strong coupling regime ($\gamma_0 = 5\lambda$), QD (blue solid line) and GQD (red solid line) versus $\gamma_0 t$ for $J = 0$, with $N = 2, 4, 6$, respectively. (d)–(f) Same as the upper panel but for $J = 0.5$.

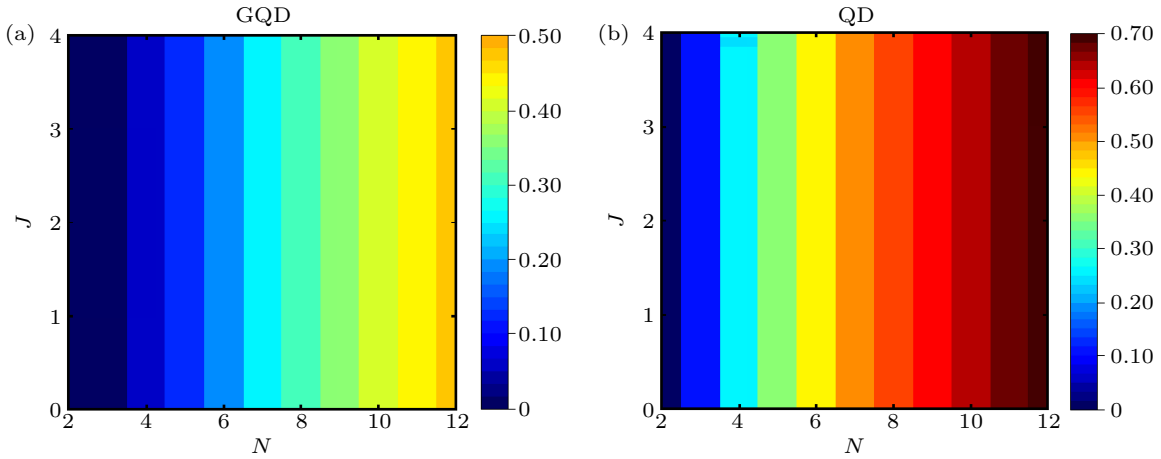


Fig. 3. (a)–(b) Under the strong coupling regime $\gamma_0 = 5\lambda$, the steady state GQD and QD serve as a function of the number of qubits N and the DDI strength J between the qubits.

3.2. QD and GQD dynamics in IBRs case

In contrast to the CBR case, we find that in the IBRs case, when $J = 0$, QD and GQD are independent of N. This can be explained by Eq. (19) that $\sigma_2 = \sigma_3 = \sqrt{\lambda^2 - 2\gamma_0\lambda}$ at this moment, and the excited state amplitude is then

$$c_j(t) = c_j(0)\, \mathrm{e}^{-\frac{\lambda t}{2}} \left[\cosh\left(\frac{\sigma_2 t}{2}\right) + \sinh\left(\frac{\sigma_2 t}{2}\right)\frac{\lambda}{\sigma_2}\right], \quad (24)$$

thus the whole reduced density matrix $\rho^{j,l}$ is independent of N. According to Ref. [50], by utilizing the final value theorem in Eq. (18), the amplitudes $\tilde{c}_j(s)$ vanish and the steady state cannot be achieved generally. Therefore, we no longer focus on the steady-state properties in the following analysis.

We select $N = 4$ to depict the evolution of QD and GQD in Fig. 4 under the weak coupling regime and the strong coupling regime. In Fig. 4(a), both QD and GQD decay to zero monotonically under the weak coupling regime, but the decay speeds of QD and GQD are much slower compared to Fig. 1(b) due to the exchange of information between the multiple reservoirs and the multiqubit system. In Fig. 4(b), although the system exhibits non-Markovian behavior under the strong coupling regime, QD and GQD decay to zero compared to the CBR case shown in Fig. 2(b). Thus in the absence of the DDI between the qubits, the auxiliary qubits in the IBRs case do not contribute to the enhancement of the QD and GQD dynamics.

Furthermore, we add DDI strength $J = 0.5$ to make a comparison with the CBR case in Fig. 5. For the system with N IBRs, when increasing the number of reservoirs, we find that the dynamics of the system would become non-Markovian even under the weak coupling regime in Figs. 5(b) and 5(c).

In the presence of multiple bosonic reservoirs, the oscillation may be caused by the backflow from the environments to the system. In addition, both the amplitude and the frequency of oscillation are significantly larger than those in the CBR case. Therefore, QD and GQD can be strengthened by increasing the number of qubits and DDI strength, which is consistent with the CBR case. However, as a result of the attenuation illustrated in Fig. 5, QD and GQD of the two qubits within the multiqubit system are zero, which is inevitable in multiple reservoirs. In both cases the similarity lies in the fact that GQD is always smaller than QD in the evolution process. As a result, QD is more effective in preserving quantum correlations than GQD.

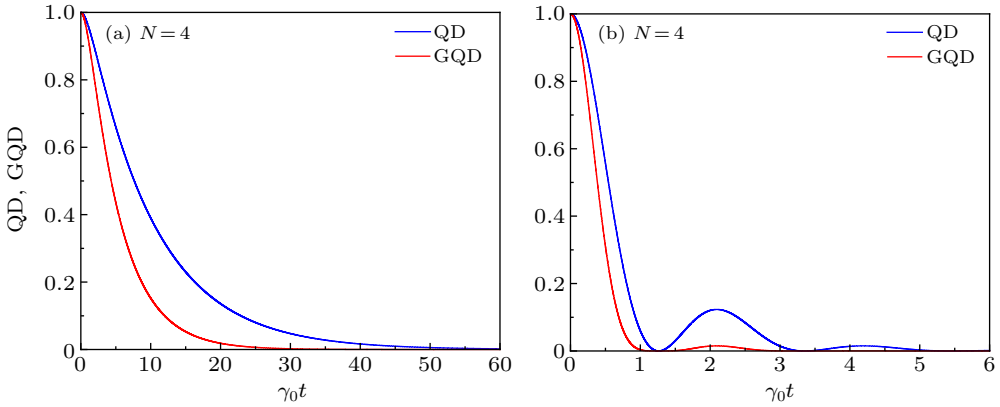


Fig. 4. QD (blue solid line) and GQD (red solid line) versus $\gamma_0 t$ for (a) weak coupling regime $\gamma_0 = 0.1\lambda$ and (b) strong coupling regime $\gamma_0 = 5\lambda$ respectively. The other parameters are fixed as $N = 4$ and $J = 0$.

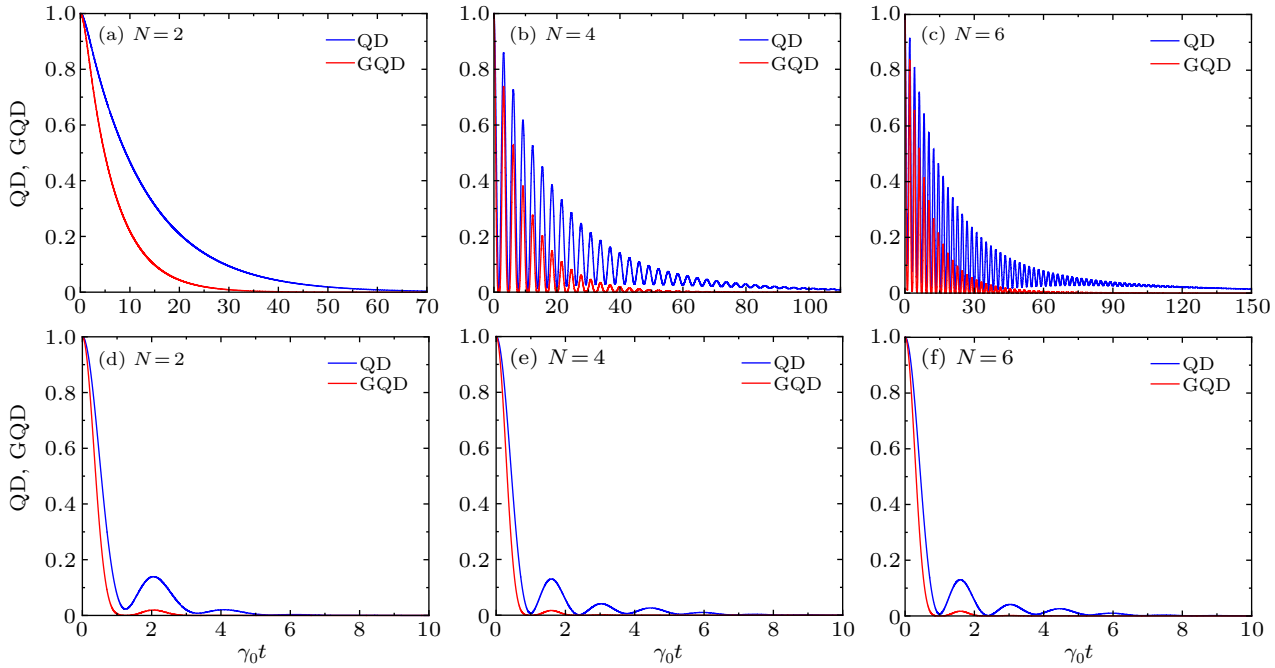


Fig. 5. (a)–(c) Under the weak coupling regime ($\gamma_0 = 0.1\lambda$), QD (blue solid line) and GQD (red solid line) versus $\gamma_0 t$ for $J = 0.5$, with $N = 2, 4, 6$, respectively. (d)–(f) Same as the upper panel but for strong coupling regime $\gamma_0 = 5\lambda$.

4. Conclusion

In summary, the dynamics and preservation of quantum correlations under the multiqubit interacting system have been thoroughly investigated. Two different correlation measurement methods were used for quantitative analysis, i.e., the QD and the GQD. The dynamical evolution of QD and GQD was assessed in two different schemes: CBR and IBRs models. The influences of the number of qubits N and DDI strength J on the dynamics of QD and GQD were also examined in detail. In the CBR case, the two-qubit QD and GQD can be strengthened with an increasing number of qubits irrespective of the presence or absence of the DDI between the qubits under the weak and strong qubit-reservoir coupling regimes. Furthermore, the two-qubit steady values of QD and GQD were determined by N in the long-time limit. These findings demonstrate that auxiliary qubits can be used to enhance QD and GQD in the multiqubit system, and that the addition of the DDI between the qubits helps preserve QD and GQD. In the IBRs

case, QD and GQD exhibited non-Markovian dynamics of the multiqubit system when $N > 2$. This means that the increasing number of qubits and reservoirs can enhance the memory effect. In addition, QD and GQD decayed more slowly than in the CBR case. And GQD was always smaller than QD during the evolution process. From these results, we conclude that QD and GQD can be preserved and strengthened by enhancing the number of qubits and the DDI strength in the CBR case. Moreover, compared to the strong coupling regime where environmental effect dominates, the increase of DDI strength J is more effective in slowing down the decay of QD and GQD in the weak coupling regime. Future studies can focus on further investigating the preservation and enhancement of quantum correlations by regulating and controlling environmental parameters.

Acknowledgments

Project supported by the National Natural Science Foundation of China (Grant Nos. 11564013 and 11964010), the Natural Science Foundation of Hunan Province (Grant No. 2020JJ4495), and the Scientific Research Fund of Hunan Provincial Education Department, China (Grant Nos. 22A0377 and 21A0333).

References

[1] Breuer H P and Petruccione F 2007 *The Theory of Open Quantum Systems* (Oxford University Press)
[2] Ollivier H and Zurek W H 2001 *Phys. Rev. Lett.* **88** 017901
[3] Baumgratz T, Cramer M and Plenio M B 2014 *Phys. Rev. Lett.* **113** 140401
[4] Datta A 2009 *Phys. Rev. A* **80** 052304
[5] Li J Q and Liang J Q 2011 *Phys. Lett. A* **375** 1496
[6] Modi K, Brodutch A, Cable H, Paterek T and Vedral V 2012 *Rev. Mod. Phys.* **84** 1655
[7] EI Anouz K, EI Aouadi I, EI Allati A and Mourabit T 2020 *Int. J. Mod. Phys. B* **34** 2050093
[8] Xing L L, Yang H, Zhang G and Kong M 2024 *Chin. Phys. B* **33** 050304
[9] Seddik S, El Anouz K and El Allati A 2022 *Int. J. Geom. Methods M.* **19** 2250025
[10] Datta A, Shaji A and Caves C M 2008 *Phys. Rev. Lett.* **100** 050502
[11] Goettems E I, Maciel T O, Soares-Pinto D O and Duzzioni E I 2021 *Phys. Rev. A* **103** 042416
[12] Adesso G, D'Ambrosio V, Nagali E, Piani M and Sciarrino F 2014 *Phys. Rev. Lett.* **112** 140501
[13] Asthana S, Bala R and Ravishankar V 2022 *Quantum Inf. Process.* **21** 35
[14] Faba J, Martín V and Robledo L 2021 *Phys. Rev. A* **103** 032426
[15] Radhakrishnan C, Laurière M and Byrnes T 2020 *Phys. Rev. Lett.* **124** 110401
[16] Wang Y, Hao L, Cheng C, Sun Y and Ma R 2024 *Int. J. Theor. Phys.* **63** 279
[17] Schlosshauer M 2019 *Phys. Rep.* **831** 1
[18] Henderson L and Vedral V 2001 *J. Phys. A* **34** 6899
[19] Dakić B, Vedral V and Brukner Č 2010 *Phys. Rev. Lett.* **105** 190502
[20] Hu X, Fan H, Zhou D L and Liu W M 2013 *Phys. Rev. A* **87** 032340
[21] Tufarelli T, Girolami D, Vasile R, Bose S and Adesso G 2012 *Phys. Rev. A* **86** 052326
[22] Piani M 2012 *Phys. Rev. A* **86** 034101
[23] De Chiara G and Sanpera A 2018 *Rep. Prog. Phys.* **81** 074002
[24] Zhou X and Zheng Z J 2022 *Eur. Phys. J. Plus* **137** 625
[25] Zhang Q, Xia Y J and Man Z X 2023 *Phys. Rev. A* **108** 062211
[26] Sinayskiy I, Ferraro E, Napoli A, Messina A and Petruccione F 2009 *J. Phys. A: Math. Theor.* **42** 485301
[27] Liao J Q, Huang J F and Kuang L M 2011 *Phys. Rev. A* **83** 052110
[28] Wang Z, Wu W and Wang J 2019 *Phys. Rev. A* **99** 042320
[29] Breuer H-P, Kappler B and Petruccione F 1999 *Phys. Rev. A* **59** 1633
[30] Sun J Y, Xu K and Li Z D 2024 *Phys. Rev. Res.* **6** 013317
[31] Fleming C H, Cummings N I, Anastopoulos C and Hu B L 2012 *J. Phys. A: Math. Theor.* **45** 065301
[32] Zhao W J, Xu K, Sun J Y, Zai D L and Wu M L 2024 *Phys. Scr.* **99** 065104
[33] Schliemann J, Khaetskii A and Loss D 2003 *J. Phys. Condens. Matter* **15** R1809
[34] Malinowski F K, Martins F, Smith T B, Bartlett S. D, Doherty A C, Nissen P D and Kuemmeth F 2018 *Phys. Rev. X* **8** 011045
[35] Vandersypen L M K, Bluhm H, Clarke J S, Dzurak A S, Ishihara R, Morello A and Veldhorst M 2017 *npj Quantum Inform.* **3** 34
[36] Fazio R and van der Zant H 2001 *Phys. Rep.* **355** 235
[37] Feng W, Zhang G Q, Su Q P, Zhang J X and Yang C P 2022 *Phys. Rev. Appl.* **18** 064036
[38] Roy T, Chand M, Bhattacharjee A, Hazra S, Kundu S, Damle and Vijay R 2018 *Phys. Rev. A* **98** 052318
[39] Manatuly A, Niedenzu W, Román-Ancheyta R, Çakmak B, Müstecaplioglu Ö E and Kurizki G 2019 *Phys. Rev. E* **99** 042145
[40] Moon G, Heo M S, Kim Y, Noh H R and Jhe W 2017 *Phys. Rep.* **698** 1
[41] Bosman S J, Gely M F, Singh V, Bruno A, Bothner D and Steele G A 2017 *npj Quantum Inform.* **3** 46
[42] Kubo K, Ho Y and Goto H 2024 *Phys. Rev. Appl.* **22** 024057
[43] Dunnett A J and Chin A W 2021 *Front. Chem.* **8** 600731
[44] Bai S Y and An J H 2021 *Phys. Rev. Lett.* **127** 083602
[45] Liang Z, Li J and Wu Y 2023 *Phys. Rev. A* **107** 033701
[46] Jiang D K, Zhang R, Liu Y and Kuang L M 2024 *Ann. Phys.-Berlin* 2400179
[47] Luo J X and Guo Q 2024 *Chin. Phys. B* **33** 060303
[48] Xiong C H, Qi W T, Miao M K and Wu M H 2023 *Chin. Phys. B* **32** 100301
[49] Bai X Y and Zhang S Y 2022 *Chin. Phys. B* **31** 040308
[50] Burgess A and Florescu M 2022 *Phys. Rev. A* **105** 062207
[51] Hu Z X, Head-Marsden K, Mazziotti D A, Narang P and Kais S 2022 *Quantum* **6** 726
[52] Chávez-Huerta M and Rojas F 2022 *Quantum Inf. Process.* **21** 347
[53] Ullah A and Dral P O 2022 *Nat. Commun.* **13** 1930
[54] Gallina F, Bruschi M and Fresch B 2022 *New J. Phys.* **24** 023039
[55] Luo S 2008 *Phys. Rev. A* **77** 42303
[56] Fanchini F F, Werlang T, Brasil C A and Arruda L G E 2010 *Phys. Rev. A* **81** 052107
[57] Altintas F 2010 *Opt. Commun.* **283** 5264